Nonlinear dynamic analysis with an uncertain computational model for mistuned bladed disks

Evangéline Capiez-Lernout, Christian Soize, Moustapha Mbaye

Florence, Italy 12-16 July 2015
ICSV22
The 22nd International Congress on Sound and Vibration

NONLINEAR DYNAMIC ANALYSIS WITH AN UNCERTAIN COMPUTATIONAL MODEL FOR MISTUNED BLADED DISKS.

Evangéline Capiez-Lernout, Christian Soize
Université Paris-Est, Laboratoire Modélisation et Simulation Multi-Échelle, MSME UMR 8208 CNRS, 5 bd Descartes, 77454 Marne-la-Vallée Cedex 02, France
email: evangeline.capiez-lernout@u-pem.fr

Moustapha Mbaye
Turbomeca - Safran Group, 64511 Bordes, Frances

This paper deals with the dynamical analysis and uncertainty quantification of a mistuned industrial rotating integrally bladed disk, for which the operating regime under consideration takes into account the nonlinear geometric effects induced by large displacements and deformations. First, a dedicated mean nonlinear reduced-order model of the tuned structure is explicitly constructed using three-dimensional solid finite elements. The random nature of the mistuning is then modeled by using the nonparametric probabilistic approach extended to the nonlinear geometric context. A stochastic reduced-order model is then obtained, which leads for solving a reasonable number of uncertain nonlinear coupled differential equations in the time domain.Such a computational strategy provides an efficient tool, which is applied to a computational model of an industrial centrifugal compressor with a large number of degrees of freedom. This allows for putting in evidence some new complex dynamical behaviors. Indeed, some complex mechanisms can be observed for the energy transfer through both geometric nonlinearities and mistuning uncertainties outside the frequency band of excitation. A careful and detailed analysis is carried out because unexpected dangerous situations, which can alter the life duration of the bladed disks, can potentially exist.

1. Introduction

In general, the natural cyclic symmetry of turbomachinery bladed disks is broken because of manufacturing tolerances and material dispersions, which create small variations from one blade to another one. Such phenomena, referred to mistuning, can generate localization effects combined to a dynamic amplification of the forced response [1]. Many research efforts have been carried out on this subject, including reduced-order models with probabilistic approaches in the numerical modeling, for taking into account the random character of mistuning [2, 3] and giving rise to strategies for the robust design of such structures [4]. Another essential aspect is to consider the geometric nonlinear effects in the computational models occurring when exceptional operating speeds of bladed disks are analyzed due to geometric nonlinearities induced by large deformations and large displacements [5, 6]. Such situation is realistic when considering a flutter kind phenomenon induced by unsteady aerodynamic coupling and yielding low damping levels. Since the unsteady aerodynamic coupling

is not considered in this paper, the nonlinear domain is simulated by increasing the magnitude of the external load, while performing forced response calculations.

The present paper proposes a methodology adapted to geometric nonlinear analysis of mistuned bladed disks combined with an industrial realistic application. The first part is devoted to the development of an adapted nonlinear reduced-order computational model for the tuned structure, referred as the mean NL-ROM. It is explicitly constructed in the context of three-dimensional solid finite elements [7] by using an appropriate projection basis [8] obtained here by a linear tuned eigenvalue analysis. Once the mean NL-ROM is established, mistuning is taken into account by implementing uncertainties through the nonparametric probabilistic framework [9, 10].

The paper is organized as follows. Section 2 describes the computational methodology and the computational aspects allowing the nonlinear dynamic analysis of mistuned rotating bladed-disks to be performed. Section 3 is devoted to the application, consisting of a finite-element model of an industrial integrated bladed disk with about 2, 000, 000 dof. The geometric nonlinear effects are analyzed and quantified through the dynamic analysis of the magnification factor in both tuned and mistuned cases.

2. Methodology

This Section is devoted to the construction of a methodology for the nonlinear mistuning analysis occurring in rotating bladed-disks structures. In the present research, the bladed-disks under consideration are assumed (1) to be made up of a linear elastic material and (2) to undergo large displacements and large deformations inducing geometric nonlinearities.

2.1 Nonlinear dynamics of a tuned bladed-disk

The tuned bladed-disk structure has an N-order cyclic symmetry. Thus, the geometrical domain, the material constitutive equation and the boundary conditions related to the generating sector are invariant under the $2\pi/N$ rotation around its axis of symmetry. Moreover, the bladed disk undergoes a rotational motion around the axis of symmetry with constant angular speed Ω. A total Lagrangian formulation is chosen, which means that the dynamical equations are expressed in the rotating frame of an equilibrium configuration considered as a prestressed static configuration.

The mean (or nominal) computational model of the tuned bladed-disk, which is constructed by the finite element method (FEM) is written as

$$
\begin{aligned}
(1) \qquad [M]\,\ddot{\mathbf{u}} + ([C(\Omega)] + [D])\,\dot{\mathbf{u}} + [K(\Omega)]\,\mathbf{u} + \mathbf{f}^{\mathrm{NL}}(\mathbf{u}) &= \mathbf{f} \quad , \\
[K(\Omega)] &= [K_e] + [K_g] + [K_c(\Omega)] \quad ,
\end{aligned}
$$

in which the $\mathbb{R}^n$-vector $\mathbf{f}$ corresponds to the finite element discretization of the external force fields, which are derived from the Lagrangian transport into the reference configuration of the physical body/surface force fields applied in the deformed configuration. The external load can represent, for instance, the unsteady pressures applied to the blades. In Eq. (1), the $\mathbb{R}^n$-vector $\mathbf{u}$ corresponds to the finite element discretization of the unknown displacement field expressed with respect to the reference configuration. In Eq. (1), the matrices $[M]$, $[D]$, $[K_g]$ and $[K_e]$ are the mass, damping, geometrical stiffness and elastic stiffness real matrices with positive definiteness property. The rotational effects are taken into account through the gyroscopic coupling matrix $[C(\Omega)]$ and the centrifugal stiffness matrix $[K_c(\Omega)]$, with antisymmetry property and with negative definiteness property respectively. It should be noted that all these matrices are also N-block circulant matrices since the structure has an N-order cyclic symmetry. The geometric nonlinearities effects are taken into account through the $\mathbb{R}^n$-vector $\mathbf{f}^{\mathrm{NL}}(\mathbf{u})$ which includes both quadratic and cubic stiffness terms. Furthermore, the centrifugal effects are assumed to be sufficiently small so that the linear stiffness matrix $[K(\Omega)]$ is positive definite, yielding only stable dynamical systems to be considered.

In the present case, the presence of the geometric nonlinearity naturally yields the nonlinear equations to be solved in the time domain, the frequency content of the nonlinear response being *a posteriori* post-analyzed by Fourier transform. The external load is defined in the time domain corresponding to a uniform sweep of a chosen frequency band of excitation. Let $\widetilde{\mathbb{B}}_s = -\mathbb{B}_s \cup \mathbb{B}_s$ be the frequency band of excitation with central frequency $s\Delta\,\nu$ and bandwidth $\Delta\nu$ defined by $\mathbb{B}_s = [(s-1/2)\Delta\nu, (s+1/2)\Delta\nu]$. The external load is written as

$$\mathbf{f}(t) = f_0\, g(t)\, \boldsymbol{\alpha} \quad , \tag{2}$$

in which f_0 is a coefficient characterizing the global load intensity, and where $\boldsymbol{\alpha}$ is an $\mathbb{R}^n$-vector corresponding to the spatial discretization of the load. In Eq. (2), the function $g(t)$ is chosen as

$$g(t) = (2\Delta\nu)\, sinc_\pi(t\Delta\nu)\, \cos(2\,\pi\, s\, \Delta\nu\, t) \quad , \tag{3}$$

where $x \mapsto sinc_\pi(x)$ is the function defined by $sinc_\pi(x) = sin(\pi\, x)/(\pi\, x)$. It should be noted that all the frequencies of the frequency band of excitation are simultaneously excited so that only one nonlinear time-domain analysis is carried out. With such a time-domain excitation, a forced-response problem is considered and not a time evolution problem with initial conditions. The considered forced-response problem is thus approximated by an equivalent time-evolution problem with zero initial conditions over a finite time interval, which includes almost all of the signal energy of the excitation. The use of the cyclic symmetry property for decomposing the nonlinear response according to its harmonic components is not considered because all the harmonic components are coupled through the geometric nonlinearity, and does not allow the problem on a single generator sector to be solved. Moreover, the full computation of the solution of the nonlinear equation defined by Eq. (1) induces a large computational effort, when dealing with realistic models of bladed-disks corresponding to a large number of DOF. Consequently, for large computational models, a reduced-order model strategy is used, and is adapted to the geometric nonlinear context under consideration (see [11, 7] and [8] for a complete overview). Let a given vector basis be represented by the $(n \times P)$ real matrix $[\Phi]$. The nonlinear response $\mathbf{u}$ is expanded as

$$\mathbf{u} = [\Phi]\, \mathbf{q} \quad , \tag{4}$$

in which $\mathbf{q}$ is the $\mathbb{R}^P$-vector of the generalized coordinates. Replacing Eq. (4) into Eq. (1) yields a nonlinear reduced set of P coupled differential equations for which all linear, quadratic and cubic terms have to be known. In the present research, the construction of the operators of such mean nonlinear reduced-order model (mean NL-ROM) is explicitly carried out in the context of the three-dimensional finite element method. It is assumed that the finite elements are isoparametric solid finite elements with 8 nodes, and using a numerical integration with 8 Gauss integration points. The elementary internal forces projected on the chosen vector basis are numerically constructed for each finite element before performing its assembly and computing all linear and nonlinear reduced operators. The detailed procedure, which also uses the symmetry properties of the linear and nonlinear reduced operators combined with distributed computations, can be found in [11]. It should be noted that each type of reduced operator is separately modeled, keeping open the possibility of implementing uncertainties issued from independent physical sources.

2.2 Nonlinear analysis of a mistuned bladed-disk

The random nature of the mistuning is then considered by implementing the nonparametric probabilistic approach, which presents the ability to include both the system-parameter uncertainties and the model uncertainties induced by modeling errors (see [9] for a complete review on the subject). It consists in replacing the operators of the mean NL-ROM by random operators, whose probability distribution is derived from the maximum entropy principle.

Let $[\mathcal{A}]$ be a $(Q \times Q)$ matrix issued from the mean NL-ROM. The corresponding random matrix $[\boldsymbol{\mathcal{A}}]$ is then written as $[\boldsymbol{\mathcal{A}}] = [U_A]\,[L_A]^T\,[\mathbf{G}_A]\,[L_A]$, where $[\mathbf{G}_A]$ is a $(Q \times Q)$ random positive-definite

matrix whose probability model is issued from the MaxEnt principle [10]. When $[\mathcal{A}]$ is a mean reduced operator with positive-definite property, representing either the mass, damping, geometrical stiffness or the opposite of the centrifugal stiffness, we have $Q = P$. When $[\mathcal{A}]$ is the mean reduced positive-definite operator issued from the reshaping of the linear elastic, quadratic and cubic stiffness as shown in [12], we have $Q = P(P+1)$. For these cases the $(Q \times Q)$ matrix $[L_A]$ is issued from the Cholesky factorization of $[\mathcal{A}]$ and matrix $[U_A]$ is the $(Q \times Q)$ identity matrix. When $[\mathcal{A}]$ is a mean reduced operator with antisymmetry property such that the gyroscopic coupling matrix, the matrices $[U_A]$ and $[L_A]$ are the $(P \times P)$ matrices defined by $[L_A] = [S_A]^{1/2}\,[B_A]^T$ and $[U_A] = [\mathcal{A}]\,[B_A]\,[S_A]\,[B_A]^T$, in which the $(P \times P)$ full and diagonal matrices $[B_A]$ and $[S_A]$ are issued from the single value decomposition (SVD) of operator $[\mathcal{A}]$. The dispersion of each random operator is then characterized by one scalar hyperparameter. Consequently, the mistuning level of the bladed-disk is entirely controlled by the $\mathbb{R}^6$-vector $\boldsymbol{\delta} = (\delta_M, \delta_D, \delta_C, \delta_{K_g}, \delta_{K_c}, \delta_K)$, belonging to an admissible set.

3. Numerical application : industrial centrifugal compressor

The structure under consideration in an industrial centrifugal compressor belonging to the class of integrated bladed disks. Due to proprietary reasons, the number M of blades characterizing the order of the cyclic symmetry of the structure cannot given. The finite element model of the structure is constructed with solid finite elements and is constituted of about $2,000,000$ degrees of freedom. Fig. 1 displays a part of the finite element mesh of the investigated bladed disk. The structure is in rotation around its revolution axis with a constant velocity $\Omega = 30,750\,rpm$. Since the dynamic analysis is carried out in the rotating frame of the structure, the rigid body motion due to the rotation of the structure corresponds to a fixed boundary condition at the inner radius of the structure. The bladed disk is made up of a homogeneous isotropic material. A modal damping model is added for the bladed disk.

Figure 1: Finite element mesh of a part of the structure

3.1 Nonlinear analysis for the tuned bladed disk

The cyclic symmetry is used for constructing the reduced matrices of the mean linear reduced-order model (MEAN-L-ROM). Let ν_0 be the first eigenfrequency. In the application, a $5-th$ engine-order excitation located at the tip of each blade is considered. The excitation frequency band is chosen such that $\mathbb{B}_e^2 = [1.78\,,\,2.34]$ and is characterized by function $g(t)$ defined with parameters $s = 4$, $\dfrac{\Delta\nu}{\nu_0} = 0.51$ from the initial time $\nu_0\,t_{ini} = -11.79$ and with a time duration $\nu_0\,T = 184$.

The chosen observation is the displacement $u_j(t)$ corresponding to the out-plane displacement located at the tip of each blade j. Let $k_0 = \arg\max_j\,(\max_{\nu/\nu_0\in\mathbb{B}}\,\widehat{u}_j^{\,\mathrm{NL}}(2\pi\nu))$ for which $\widehat{u}_j^{\,\mathrm{NL}}(2\pi\nu)$ is the Fourier transform of $u_j^{\mathrm{NL}}(t)$. In the frequency domain, the observation $w(2\pi\nu)$ corresponding to the selected blade out-plane displacement is defined by $w(2\pi\nu) = \widehat{u}_{k_0}(2\pi\nu)$. Figure 2 displays

the graphs $\nu/\nu_0 \mapsto w^{\mathrm{L}}(2\pi\nu)$ (upper graph) and $\nu/\nu_0 \mapsto w^{\mathrm{NL}}(2\pi\nu)$ (lower graph) corresponding to a load intensity $f_0 = 2.5\,N$. The spreading of the vibrational energy over the whole frequency band of analysis $\mathbb{B}$ is due to the nonlinear geometric effects and is characterized through secondary response peaks. For high frequencies that are located outside $\mathbb{B}_e^2$ in dimensionless frequency band $[3\,,\,3.34]$, the dynamical response induced by the geometric nonlinearities is negligible. Nevertheless, some new resonances appear with the same order of magnitude than the main resonance in the dimensionless frequency band $\mathbb{B}_{sub} = [1\,,\,1.5]$(Note that, in this band, there exist several tuned eigenfrequencies of the structure, which are only excited through the chosen excitation under the linear assumption). We put then in evidence a complex dynamical behavior that can be dangerous because non-expected resonances with non-negligible amplitudes appear outside excitation frequency band $\mathbb{B}_e^2$.

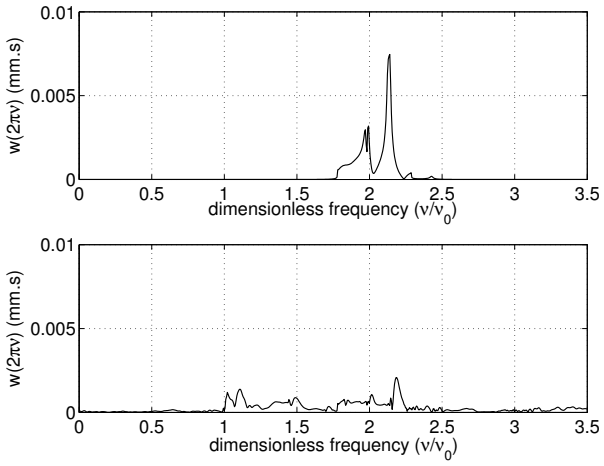

Figure 2: Frequency domain observation $\nu/\nu_0 \mapsto w(2\pi\nu)$ related to the linear (upper graph) and the nonlinear (lower graph) cases for $\mathbb{B}_e^2 = [1.78\,,\,2.34]$ and $f_0 = 2.5\,N$.

Figure 3 displays the graphs $\nu/\nu_0 \mapsto w^{\mathrm{L}}(2\pi\nu)$ (upper graph) and $\nu/\nu_0 \mapsto w^{\mathrm{NL}}(2\pi\nu)$ (lower graph) corresponding to a load intensity $f_0 = 2.75\,N$. It can be seen that the main resonance amplitude is nearly twice the resonance amplitude located in $\mathbb{B}_e^2$. Moreover, a broad range of frequency band $\mathbb{B}_{sub} = [1\,,\,1.5]$ is excited, yielding a large number of resonances with the same order of magnitude than the resonance amplitudes located in $\mathbb{B}_e^2$.

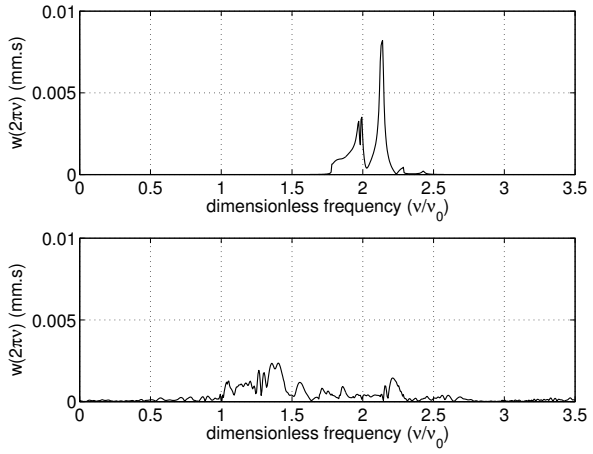

Figure 3: Frequency domain observation $\nu/\nu_0 \mapsto w(2\pi\nu)$ related to the linear (upper graph) and the nonlinear (lower graph) cases for $\mathbb{B}_e^2 = [1.78\,,\,2.34]$ and $f_0 = 2.75\,N$.

3.2 Nonlinear analysis for the mistuned bladed disk

In the present case, the MEAN-NL-ROM is constructed by modal analysis without substructuring techniques. The uncertainties are not considered as independent from one blade to another one, which is coherent with the structure under consideration belonging to the class of integrated bladed disks, that are manufactured from a unique solid piece of metal. In the present analysis, for a better understanding of the phenomenon, only the matrices related to the linear part are random. The mistuning level is thus controlled by the $\mathbb{R}^5$-vector $\boldsymbol{\delta} = (\delta_M, \delta_D, \delta_C, \delta_{K_c}, \delta_K)$. The analysis is focussed for the excitation frequency band $\mathbb{B}_e^2$ that exhibits the complex dynamic situation described above. The load intensity is fixed to $f_0 = 2.5\,N$ and the uncertainty level is set to $\boldsymbol{\delta} = (\delta_M, \delta_D, \delta_C, \delta_{K_c}, \delta_K) = (\delta, 0.2, 0.2, 0.2, \delta)$, in which $\delta = \delta_M = \delta_K$. Thus, the effects of mass and elastic uncertainties combined to uncertainties for the rotational effects are taken into account in the analysis. For fixed $\nu/\nu_0 \in \mathbb{B}$, let $Y(2\pi\nu)$ be the random dynamic amplification factor defined by

$$Y(2\pi\nu) = \frac{W(2\pi\nu)}{\max_{\nu/\nu_0 \in \mathbb{B}} w(2\pi\nu)} \quad . \tag{5}$$

Figures 4 shows the confidence region of the nonlinear observation $Y^{\mathrm{NL}}(2\pi\nu)$ for $\delta = 0.02$. It is seen that the extreme values related to $Y^{\mathrm{NL}}(2\pi\nu)$ yield moderate amplification even if the confidence region remains relatively broad. Although not presented in the present paper, it can be shown that, on the contrary, the linearized assumption clearly increases this amplification. It can then be deduced that the geometric nonlinear effects clearly inhibit the amplification of the random response.

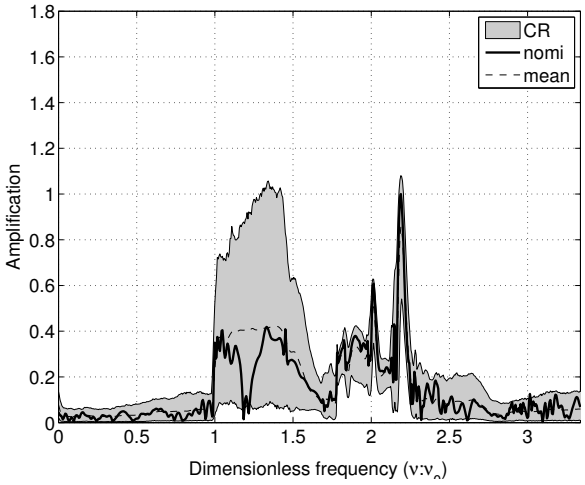

Figure 4: Stochastic analysis: frequency domain observation $Y^{\mathrm{NL}}(2\pi\nu)$ related to the nonlinear case for $\delta_K = \delta_M = 0.02$ and for $\delta_{K_c} = \delta_C = \delta_D = 0.2$: mean model (thick line), mean of the stochastic model (thin dashed line), confidence region (gray region).

From now on, the analysis is focussed on the quantification of the amplification with respect to δ. Let Y_∞ be the random amplification factor defined by $Y_\infty = \max_{\nu/\nu_0 \in \mathbb{B}} Y(2\pi\nu)$. We then define the second random amplification factor, Z_∞, such that

$$Z_\infty = \frac{\max_{\nu/\nu_0 \in \mathbb{B}_{sub}} W(2\pi\nu)}{\max_{\nu/\nu_0 \in \mathbb{B}_{sub}} w(2\pi\nu)} \quad . \tag{6}$$

Figure 5 displays the probability density function of Y_∞^{NL} for several values of δ. It can clearly be seen that the probability density functions (pdf) exhibit a support that is $[0.55\,,\,1.5]$. These pdf are not symmetric, yielding amplification factors greater than 1 with a lower probability level. Furthermore,

from $\delta \geq 0.23$, the shape of the pdfs seems to be less sensitive to the level of uncertainties. Figure 6 displays the pdfs of Z_{∞}^{NL} for several values of δ. The pdfs exhibit a support that is $[0.55\,,\,3.3]$. It then points out, not only a complex sensitivity to uncertainties, but also high amplification levels with respect to secondary resonances that correspond to unexpected amplifications.

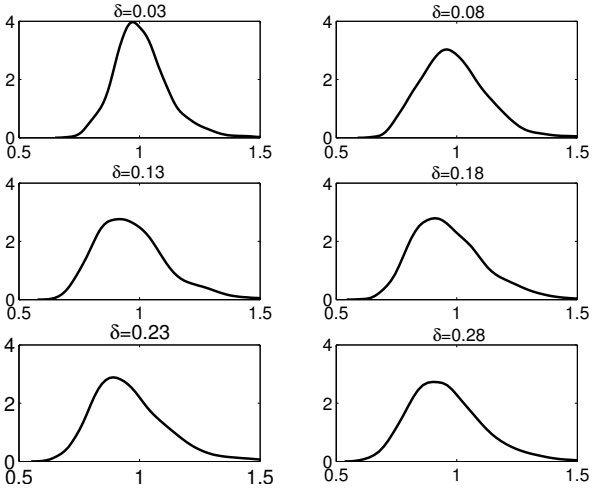

Figure 5: Probability density function $p \mapsto Y_{\infty}^{\mathrm{NL}}(p)$ for $\delta = 0.03, 0.08, 0.13, 0.18, 0.23, 0.28$.

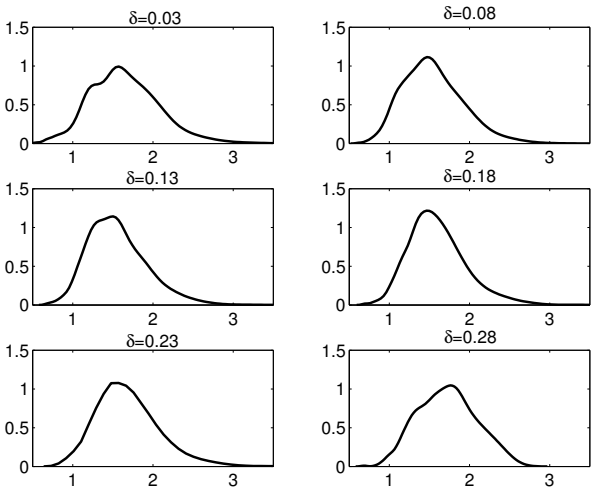

Figure 6: Probability density function $p \mapsto Z_{\infty}^{\mathrm{NL}}(p)$ for $\delta = 0.03, 0.08, 0.13, 0.18, 0.23, 0.28$.

4. Conclusion

The paper has presented an analysis of the geometric nonlinear effects of an uncertain mistuned rotating industrial integrated bladed disk subjected to a high loading level. The numerical results presented display new complex dynamical behaviors of the dynamical response of the blades.

The nonlinear tuned response is shown to be spread outside the frequency band of excitation, yielding secondary resonances corresponding to sub-harmonics whose contribution cannot be longer neglected. Considering the nonlinear mistuned response with uncertainties, the geometric nonlinear effects play an important role for the propagation of uncertainties. In particular, the robustness of the random response with respect to uncertainties remains strong in the frequency band of excitation,

yielding reasonable amplification levels. However, such robustness suddenly falls in the sub-harmonic frequency range giving rise to consequent local amplification levels.

In summary, all the numerical results have demonstrated that the life duration of the industrial bladed disk can be very sensitive to the presence of geometric nonlinearities combined with mistuning effects.

5. Acknowledgements

This work was supported by the DGA (French defence procurement agency) in the context of the TURBODYNA project (project number ANR-13-ASTR-0008-01) related to the ANR ASTRID research program (specific support scheme for research works and innovation defence). SAFRAN Turbomeca is also acknowledged for giving permission to publish this work.

REFERENCES

1. S.-T. Wei and C. Pierre, *Localization Phenomena in Mistuned Assemblies with Cyclic Symmetry Part II: Forced Vibrations*, ASME Journal of Vibration, Acoustics Stress and Reliability in Design, Vol. 110(4), (1988) pp. 439-449.

2. E. Capiez-Lernout, C. Soize, *Nonparametric modeling of random uncertainties for dynamic response of mistuned bladed disks*, ASME Journal of Engineering Gas, Turbine and Power, Vol.126(3), (2004), pp. 610-618.

3. M. Mbaye, C. Soize, J. Ousty, *A reduced-order model of detuned cyclic dynamical systems with geometric modifications using a basis of cyclic modes*, ASME Journal of Engineering for Gas Turbines and Power, Vol.132(11), (2010), paper 112502.

4. M. Mbaye, C. Soize, J. Ousty, E. Capiez-Lernout, *Robust Analysis of Design in Vibration of Turbomachines*, ASME Journal of Turbomachinery, Vol.135(2), (2013), paper 021008.

5. A.F. Vakakis, *Dynamics of a nonlinear periodic structure with cyclic symmetry*, Acta Mechanica, Vol.95(1-4), (1992), pp. 197-226.

6. A. Grolet, F. Thouverez, *Vibration analysis of a nonlinear system with cyclic symmetry*, ASME Journal of Engineering for Gas Turbines and Power, Vol.133(2), (2011), paper 022502.

7. E. Capiez-Lernout, C. Soize, M.-P. Mignolet, *Post-buckling nonlinear static and dynamical analyses of uncertain cylindrical shells and experimental validation* Computer Methods in Applied Mechanics and Engineering, Vol. 271, (2014), pp. 210-230.

8. M.-P. Mignolet, A. Przekop, S.A. Rizzi, M.S. Spottswood, *A review of indirect/non-intrusive reduced-order modeling of nonlinear geometric structures*, Journal of Sound and Vibration, Vol.332(10), (2013), pp. 2437-2460.

9. C. Soize, *Stochastic Models of Uncertainties in Computational Mechanics*, Lecture Notes in Engineering Mechanics 2, American Society of Civil Engineers (ASCE) (2012).

10. C. Soize, *Random matrix theory for modeling uncertainties in computational mechanics*, Computer Methods in Applied Mechanics and Engineering, Vol. 194(12-16), (2005), pp. 1333-1366.

11. E. Capiez-Lernout, C. Soize, M.-P. Mignolet, *Computational stochastic statics of an uncertain curved structure with geometrical nonlinearity in three-dimensional elasticity* Computational Mechanics, Vol. 49(1), (2012), pp. 87-97.

12. M.-P. Mignolet, C. Soize, *Stochastic reduced-order models for uncertain geometrically nonlinear dynamical systems*, Computer Methods in Applied Mechanics and Engineering, Vol. 197, (2008), pp. 3951-3963.